Chemical Engineering Journal 138 (2008) 425–435

Chemical Engineering Journal

www.elsevier.com/locate/cej

Hydrodynamics of a liquid–solid circulating fluidized bed: Effect of dynamic leak

S. Vidyasagar, K. Krishnaiah, P.S.T. Sai *

Department of Chemical Engineering, Indian Institute of Technology Madras, Chennai 600 036, India

Received 24 December 2006; received in revised form 30 May 2007; accepted 25 June 2007

Abstract

Experiments were conducted in a liquid–solid circulating fluidized bed (LSCFB) of 80 mm i.d. and 2.8 m high to study the macroscopic flow structure over a wide range of liquid velocity and solids inventory in the storage vessel. The results indicate that the valve configuration (i.e. lift pot and the angle made by the solids feed pipe with the riser), solids inventory in the storage vessel and location of the primary liquid distributor were found to play an important role on the macroscopic properties of LSCFB. Dynamic leak, flow of solids from the return leg into the riser in the absence of auxiliary liquid flow, has been noticed at very high liquid velocities when the primary liquid distributor inlet (positioned at the bottom of the riser) is near to the solids feed pipe from the storage vessel. The dynamic leak was prevented by changing the position of the primary distributor inlet and the macroscopic flow behavior with and without dynamic leak was compared. The transitional liquid velocity that demarcates the conventional fluidization from the circulating fluidization was determined by three different methods and was found to be independent of solids inventory and dynamic leak.

Keywords: Macroscopic flow; Pressure drop; Onset velocity; Transitional liquid velocity; Dynamic leak

1. Introduction

Liquid–solid circulating fluidized bed (LSCFB) consists of a riser, downcomer (or storage vessel), liquid–solid separator and other auxiliary devices. Usually the riser is operated at liquid velocities higher than the terminal velocity of the particle and the downcomer is operated at low velocities either in packed or conventional fluidized bed regime with continuous circulation of solids between the riser and the downcomer. LSCFBs enjoy number of advantages, such as they minimize the dead zone and increase the contacting efficiency between the liquid and solid phases in the riser. These advantages result in considerable increase in fractional conversion as well as the production efficiency per unit cross-sectional area of the system.

LSCFBs find potential applications in physical, chemical and biological processing [1]. In the synthesis of linear alkyl benzene [2–6], the main alkylation reaction takes place in the riser with simultaneous deactivation of the solid catalyst and the deactivated catalyst is regenerated in the downcomer by another stream. The reactivated catalyst is fed back into the riser from the downcomer. Similarly, in the case of continuous recovery of proteins from un-clarified whole broth [7–9], the adsorption and desorption (regeneration) of proteins are carried out separately in the downcomer and the riser, respectively, in a continuous mode with ion exchange particles circulated between the two columns. For the removal of biological nutrient from waste water, solid particles with biofilm are circulated between the riser where nitrification occurs and the downcomer where de-nitrification is carried out simultaneously [10].

For the development of an appropriate model and design of a liquid–solid circulating fluidized bed as a reactor or a contacting device, estimation of various transport properties, kinetic and mixing parameters are required [6,11]. The mixing characteristics and the transport properties depend strongly on the hydrodynamics. Hydrodynamics include flow regime, flow pattern of the each phase, solids circulation rate, phase holdup distribution, etc. Since the riser of a LSCFB is accompanied by the downcomer with continuous circulation of solids between them, the above hydrodynamic variables in the riser in turn will depend on the structure of the solids feeding system, liquid distributor design and solids inventory in the downcomer.

Abbreviations: LSCFB, liquid–solid circulating fluidized bed; CFB, circulating fluidized bed

* Corresponding author. Tel.: +91 44 22574163; fax: +91 44 22574152.
E-mail address: psts@iitm.ac.in (P.S.T. Sai).

1385-8947/$ – see front matter © 2007 Elsevier B.V. All rights reserved.
doi:10.1016/j.cej.2007.06.020

Nomenclature

C_D	effective drag coefficient
G_s	solids circulation rate (kg/m^2 s)
H	bed height from the auxiliary distributor plate (m)
n	Richardson and Zaki index
$\Delta P/\Delta Z$	static pressure gradient (Pa/m)
U_l	total superficial liquid velocity (m/s)
U_{l1}	primary liquid velocity or main liquid velocity (m/s)
U_{l2}	secondary liquid velocity or auxiliary liquid velocity (m/s)
U_{lc}	critical transition velocity from conventional to circulating fluidization regime (m/s)
U_{lt}	critical transition velocity from circulating to transport bed regime (m/s)
U_s	particle circulation rate expressed as superficial particle velocity (m/s)
U_{slip}	experimental slip velocity (m/s)
U_t	particle terminal velocity (m/s)

Greek letters

ε	experimental bed voidage
$\bar{\varepsilon}$	bed voidage predicted for homogeneous fluidization
ε_s	average solids holdup in the riser
$\varepsilon_{s,l}$	sectional solids holdup along the riser

For the operation of LSCFB, one needs two liquid streams at the bottom of the riser. While one stream acts as a main fluidizing media into the riser, the other regulates the solids flux from the downcomer into the bottom of the riser. Two different types of liquid distributor arrangements are reported in literature. In the first arrangement, primary liquid is sent through a pipe type distributor from the bottom of the riser and secondary liquid is sent through a distributor plate at the side of the riser [12–18]. In this arrangement, the solids feed pipe connecting the riser and downcomer makes an angle with the axis of the riser and the axis of the downcomer. In the second arrangement, the main liquid is sent through a porous plate distributor at the bottom of the riser and the other stream is sent through an L-Type valve connecting the riser and the downcomer [6,19–22].

In addition to the secondary stream, Liang et al. [12] used a third stream at high flow rates at the bottom of the downcomer for pushing the solids into the riser from the downcomer. The flow rate of the third stream was not accounted by them for calculating the hydrodynamic variables. Hence they observed the critical transitional liquid velocities to circulating fluidized bed regime much earlier than the terminal velocity of the particle. From the pressure balance on LSCFB, Zheng and Zhu [14] concluded that the solids inventory in the downcomer and solids feeding system strongly influence the solids circulation rate, solids holdup and stable operating range of LSCFB. With high solids inventory in the storage vessel, they also introduced the third stream at low flow rates at the bottom of the storage vessel to loosen up the solids to achieve stable operation. They observed, for their valve configuration, a range of solids circulation and secondary liquid velocity over which LSCFB undergoes unstable operation. Only Feng et al. [18] studied the effect of location of primary liquid distributor on the solids circulation rate and found that the location of the primary liquid distributor plays a very important role in the hydrodynamics of a LSCFB system.

Excepting due to Zheng et al. [13], Zheng and Zhu [14] and Feng et al. [18], the information available in the literature on flow behavior is restricted to one particular solids inventory in the downcomer and one particular location of primary liquid distributor. In the present investigation, experiments were conducted to study the macroscopic flow properties at various liquid velocities and solids inventory in the downcomer for two different locations of the primary liquid distributor. Experiments were also conducted to find out the transition from conventional fluidization to circulating fluidized bed regime by different experimental methods. Even though the liquid distributor arrangement of the present study is similar to the first arrangement [12,13,16,17] mentioned earlier, unstable operation was not observed. Hence it is possible to operate LSCFB with very low solids inventory without the introducing the third stream.

2. Experimental

A schematic of the experimental setup is shown in Fig. 1. It consists of a riser, liquid–solid separator, solids return pipe, downcomer (or solids storage vessel) and solids feeding pipe (or return leg).

The riser was made up of Acrylic column with an i.d. of 80 mm and o.d. of 90 mm using multiple sections. The total height of the column was 2.8 m and that of the test section from the auxiliary distributor plate was 2.2 m. The riser was provided with pressure tapings at 200 mm intervals. The pressure taps were connected to a multi-limb U-tube manometer to record the pressure drop in each section of the riser. The main liquid distributor at the bottom of the riser consists of two distributors namely, the primary and the auxiliary liquid distributors. In the primary distributor, seven stainless steel tubes of 12.7 mm i.d. extending into the riser were fixed uniformly across the cross-section of the riser to ensure uniform liquid distribution. They occupy 17.6% opening area of the riser. The auxiliary distributor was a multi-orifice SS plate with 5% opening area and provision to insert the primary distributor tubes.

The liquid pumped from the reservoir was admitted as two streams with main (or primary) liquid stream entering the riser through the primary liquid distributor and the secondary (or auxiliary) liquid stream entering through the auxiliary distributor. The upper end of the riser projects 150 mm centrally into the liquid–solid separator. The liquid–solid separator was a large cone based cylindrical acrylic vessel which allows the particles to settle down from the liquid. The liquid leaves the liquid–solid separator at the liquid outlet placed at the top of the separator to liquid reservoir. The separated solids from liquid–solid separator are returned through the solids return pipe and solids circulation rate measuring device into the storage vessel.

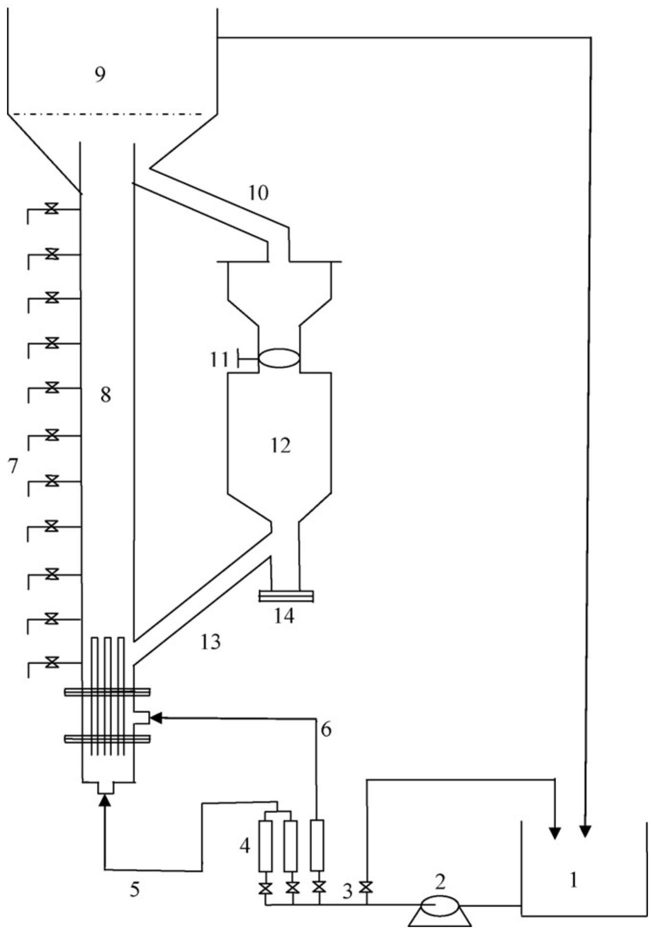

Fig. 1. Schematic of the experimental setup. 1. Liquid reservoir; 2. pump; 3. valve; 4. flow meters; 5. main liquid; 6. auxiliary liquid; 7. pressure taps; 8. riser; 9. liquid–solid separator; 10. solids return pipe; 11. butterfly valve; 12. downcomer; 13. solids feeding pipe or return leg; 14. solids-discharge.

In the solids circulation measuring device, the column wall was marked with graph paper along its length above the butterfly valve. Solids falling continuously into the downcomer were charged into the bottom of the riser by solids feeding pipe. One end of solids feeding pipe was joined to the riser well above the auxiliary liquid distributor and the other end was joined to the bottom of the conical section of the storage vessel.

In a typical experiment, the riser was initially packed with particles to a known height. The primary liquid was admitted into the column at very low liquid velocity through the calibrated flow meters. After steady state was reached, the pressure drop across the bed was noted. The primary liquid flow rate was increased in small intervals and the pressured drop was noted each time. This procedure was continued till the bed expanded to the entire length of the riser with the solids about to entrain form the top of the riser. At this condition, the secondary liquid was introduced to a particular known value and the circulation of solids between the riser and downcomer starts. Once the system has attained the steady state, the pressure drop along the length of the riser and solids circulation rate were noted. The solids circulation rate was determined by closing the butterfly valve and noting the time needed to accumulate a predetermined height of solids above the butterfly valve. The solids circulation rate measurement was repeated two to three times to ensure the accuracy. For the same auxiliary liquid flow rate, the primary liquid flow rate was increased by small increments until the transport bed regime is reached or limited by the pump capacity. For each increment of primary liquid flow rate, pressure drop along the riser and solids circulation rate were measured. This same procedure was repeated for various fixed values of auxiliary liquid flow rates and various solids inventory in the downcomer for two different locations of the primary liquid distributor.

Table 1
Range of the variables investigated in the present study

Variable	Range
Primary liquid velocity (m/s)	0–0.34
Auxiliary liquid velocity (m/s)	0.014–0.107
Particle diameter (mm)	1.36
Particle density (kg/m^3)	2468
Solids inventory (m)	0.15–0.45

The onset velocity was determined by bed emptying test. In this method, the riser was packed with solids to a known height from the primary liquid distributor and the primary liquid was introduced without the auxiliary flow. For every primary liquid velocity, the time taken to entrain all the particles above the main liquid distributor of the riser was noted down as the bed empting time. The same procedure was repeated for every increment in primary liquid velocity and for different initial heights of solids.

The glass particles with an average diameter of 1.36 mm and density of 2468 kg/m^3 was used as the dispersed phase. Tap water was used as the continuous phase. All the experiments were carried out at ambient temperature. By neglecting the effect of wall friction, the average solids holdup at each measured section was determined by measuring the pressure gradient along the riser. The range of variables investigated in the present study is detailed in Table 1.

3. Results and discussion

The function of the auxiliary liquid is to loosen up the particles in the liftpot (i.e. the space adjacent to the primary liquid distributor tubes at the bottom of the riser above the auxiliary distributor plate), push the solids up to the tip of the riser and allow the solids from the feeding pipe into the riser. With increasing the auxiliary liquid flow rate, a slow moving bed is observed in the return leg to transport the solids into the riser. Hence, solids holdup and solids circulation rate in the riser can be controlled by adjusting the ratio of primary and auxiliary liquid flow rates. Therefore, auxiliary liquid flow acts as a control device for solids circulation and solids holdup. Without any external mechanical devices, such as valves, solids circulation rate and solids holdup can be regulated by this kind of solids feeding system and hence the lift pot, auxiliary distributor and solids feeding pipe form as a non-mechanical valve [15].

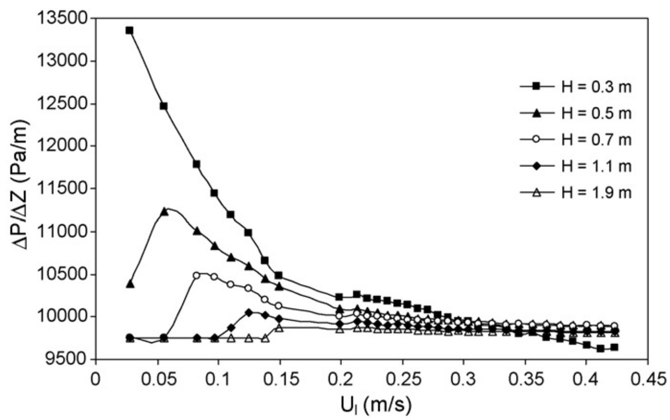

Fig. 2. Variation of pressure drop along the riser with superficial liquid velocity.

3.1. Static pressure gradient variations from conventional fluidization regime to transport regime

Fig. 2 shows the typical pressure gradient profiles along the length of the riser with total superficial liquid velocity. Pressure gradient at $H = 0.3$ m corresponds to the pressure drop measured between 0.2 and 0.4 m from the auxiliary distributor plate. The pressure gradient starts to decrease at the bottom section of the riser (at $H = 0.3$ m) with increasing the liquid velocity as solids concentration in that section decreases continuously due to the expansion of the bed. At the middle section of the riser, for example at $H = 1.1$ m, the pressure gradient is constant up to $U_l = 0.096$ m/s since the solids bed did not expand up to that section. With increasing liquid velocity beyond 0.096 m/s, the pressure gradient increases as the fluidizing solids starts entering this section. When this section between 1.0 and 1.2 m is completely occupied by the fluidizing solids (corresponding to $U_l = 0.124$ m/s) a peak in pressure gradient is observed. With further increase in liquid velocity, the fluidizing solids enter the next section. Hence the pressure gradient starts decreasing as solids concentration in that section decreases. A similar trend as above has been observed at the uppermost section of the riser (at $H = 1.9$ m). The liquid velocity at the peak of the static pressure gradient profile for this section (0.15 m/s) is defined as the critical transitional liquid velocity of the circulating fluidization regime where the solids are about to entrain out of the riser. This demarcates the boundary between conventional and circulating fluidization regimes. At this velocity of 0.15 m/s, the pressure gradient at the bottom section is still higher than at the top section and axial distribution of solids holdup exists in the riser. Beyond this velocity, the circulating fluidization regime starts in the riser with continuous circulation of solids between the riser and downcomer. The pressure gradient starts decreasing with further increase in superficial liquid velocity with the riser in circulating fluidized bed regime and at one particular velocity pressure drop profiles merge together indicating that bed is entered into transport bed regime. At this condition, the solids holdup is low with uniform axial distribution of solids in the riser. The superficial liquid velocity at which pressure drop profiles are merging together is called as the critical transitional velocity from the circulating fluidization to transport regime [17].

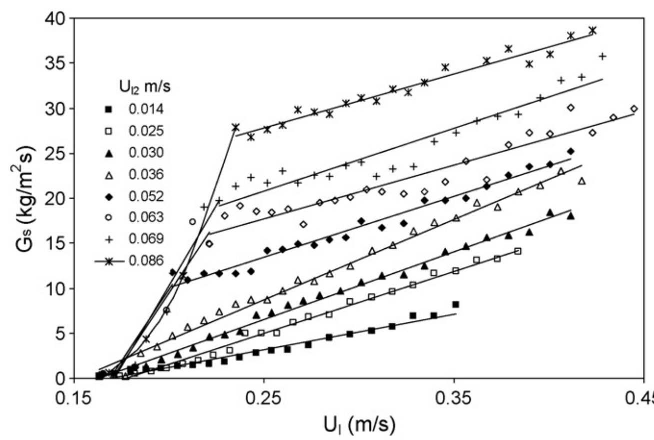

Fig. 3. Variation of solids circulation rate with liquid velocity.

These profiles are similar to that reported in the literature for the case of a gas–liquid–solid circulating fluidized beds [17,23–25] if the pressure drop due to gas phase is neglected. The pressure drop contribution due to gas phase is negligible as the gas holdup is low and the density of gas is negligible compared to liquid and solid.

3.2. Flow behavior in circulating fluidization regime

3.2.1. Effect of auxiliary liquid flow rate on average solids holdup and solids circulation rate

Fig. 3 shows the variation of solids circulation rate with total superficial liquid velocity and auxiliary liquid velocity. For a given total liquid velocity, the solids circulation rate increases with increasing auxiliary liquid velocity. This is expected since more voidage is created in the liftpot with increasing auxiliary liquid velocity and there by more particles are introduced into the riser from the return leg.

Two different types of profiles are noticed from Fig. 3. One is at the lower auxiliary liquid flow rates, i.e. up to $U_{l2} = 0.036$ m/s where the solids circulation rate is varying linearly with total superficial liquid velocity. This behavior was not observed by earlier investigators even though the solids feeding structure of the present study is nearly similar to them [12–15]. The other profile is at higher auxiliary liquid flow rates where the variation of solids circulation rate with total superficial liquid velocity can be divided into two zones: an initial zone in which the solids circulation rate increases rapidly with small increase in total liquid velocity followed by a zone in which the increase in solids circulation rate is very small.

As shown in Fig. 4, there is sufficient gap between the intersection of the riser and bottom of the solids feed pipe from the auxiliary liquid distributor (70 mm) in the experimental setup of the present study. The angle made by return leg with the riser is less (30°). Hence at lower auxiliary liquid velocity, up to $U_{l2} = 0.036$ m/s, the auxiliary liquid flows completely into the riser. In addition, the flow of solids in return leg is slow moving packed bed with small flux of solids entering into the riser and hence solids circulation varies linearly with total superficial liquid velocity.

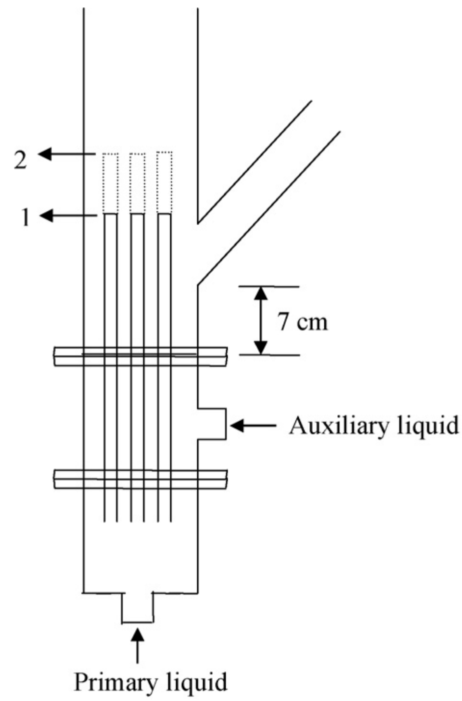

Fig. 4. Arrangement of primary liquid distributor (1. with dynamic leak; 2. without dynamic leak).

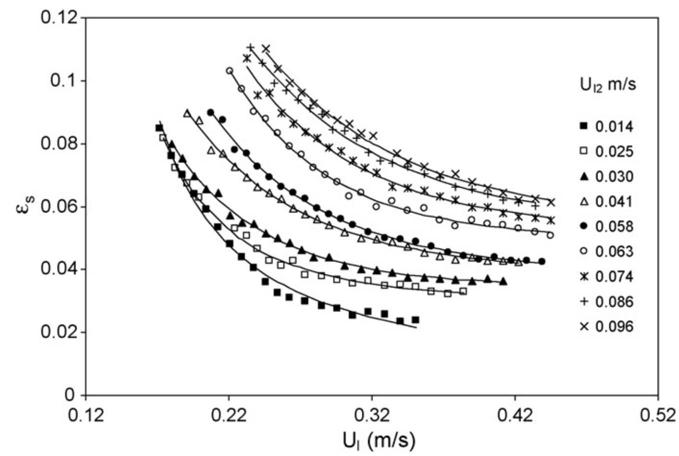

Fig. 5. Variation of solids holdup with liquid velocity.

Zheng et al. [13,15] and Zheng and Zhu [14] did not notice this linear variation at low auxiliary liquid velocities as the intersection of the return leg and riser was very near to the auxiliary distributor and the angle made by the return leg with the riser is larger in their experimental setup. Hence at low auxiliary liquid velocities, part of the liquid stream was going into the riser and the remaining through the return leg into the storage vessel. Thus the auxiliary liquid was not effectively utilized into the riser. To overcome this problem, they introduced a third stream [15] in the cone part of the storage vessel and used higher solids inventory in the downcomer (i.e. 1, 1.2 and 1.5 m). Hence higher initial auxiliary liquid velocities were needed to push the solids surrounding the tube into the tip of the tube to achieve solids circulation. In the present study, on the other hand, it is possible to operate at low auxiliary liquid velocities without third stream and with low solids inventory in the storage vessel (i.e. 0.15, 0.25 and 0.35 m). The minimum normalized auxiliary liquid velocity used by the above authors [13–15] was 0.23 where as in the present study it is 0.07. Since the particle size of the present study is different from earlier investigations [13–15], auxiliary liquid velocities are normalized with the terminal velocity for meaningful comparison.

The variation of solids circulation rate with total superficial liquid velocity at higher auxiliary velocities in the second zone (linear but not constant) is quite different from the literature [12–15]. This could be due to either variation in methods followed for solids circulation measurement or lower solid inventory in the downcomer of the present study.

According to Zheng et al. [13] and Zheng and Zhu [14], for a given total liquid velocity, there is a maximum solids circulation rate associated with an auxiliary liquid velocity beyond which the operation become unstable. This is due to pressure imbalance between the riser and storage vessel and there is a limit for minimum and maximum auxiliary liquid flow rates to achieve stable operation. For the valve configuration and with in the range of the experimental conditions of the present study, unstable operation was not observed. Hence, it can be concluded that structure of the valve configuration plays a very important role in the flow behavior of the LSCFB.

The variation of average solids holdup with the total liquid superficial velocity and auxiliary liquid velocity in the circulating fluidized bed regime is shown in the Fig. 5. For a fixed total liquid velocity, the solids holdup increases with increase in auxiliary liquid velocity. At low auxiliary velocities, there is slow moving packed bed of solids in the return leg with low solids flux entering into the riser. With increase in auxiliary liquid velocity, the flow of solids in the return pipe changes to moving bed and to transport bed with increasing solids flux into the column. Hence, for a fixed total superficial liquid velocity, solids holdup increases with increase in auxiliary liquid flow rate. This observation is similar to that reported in literature and the same explanation holds well [13,23]. At higher auxiliary liquid velocities, the variation of average solids holdup is nearly linear with increase in total superficial liquid velocity. This is because of low solids inventory and the difference in valve configuration of the present study compared to the literature.

At lower total superficial liquid velocities, solids holdup decreases quickly with increasing total liquid velocity as solids velocity increases quickly and more solids are thrown out off the riser. At higher total liquid velocities, on the other hand, the effect of liquid velocity on the solids velocity/solids circulation rate is negligible and hence solids holdup shows a plateau.

From Figs. 3 and 5, it can be concluded that average solids holdup and solid circulation rate are affected by both primary and auxiliary liquid velocity. One of the biggest advantages if LSCFB is used as reactor is that the desired solids holdup and solids velocity/solids circulation rate in the riser can be maintained at any desired values by suitably adjusting the ratio of primary and secondary liquid velocities according to the reaction requirement.

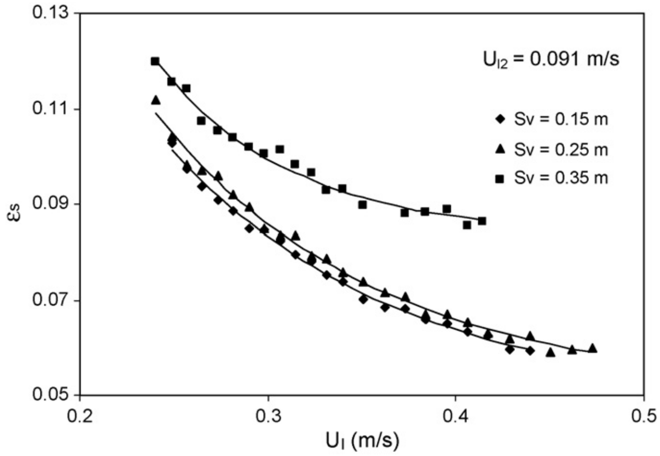

Fig. 6. Effect of total solids inventory on solids holdup.

3.2.2. *Effect of solid inventory in the downcomer on solids holdup and solids circulation rate*

For a given non-mechanical valve configuration, the solids holdup in the riser depends on the solids inventory in the downcomer. The effect of solids inventory on the average solids holdup inside the riser is shown in Fig. 6. At fixed primary and auxiliary liquid velocities, the solids holdup increases with increase in solids inventory. By increasing solids inventory, more solids are added to the downcomer and the weight of the bed acting on the return leg is larger. Hence, more solids are pushed into the riser.

From Fig. 7a and b, it can be observed that solids circulation rate is increasing with increasing solids inventory at fixed primary and auxiliary liquid velocities. Higher solids circulation rates are obtained at higher solids inventory as more weight is acting at the bottom of the downcomer and on the solids in return leg. Figs. 6 and 7 indicates that the solids inventory in the downcomer does not alter the solids holdup and solids circulation rate profiles. Hence, based on the information available in the literature [13,14] and from the present study, it can be concluded that the solids circulation rate and solids holdup in the riser are affected not only by the operating variables, such as primary and auxiliary liquid velocity, but also by the non-mechanical valve configuration.

3.2.3. *Axial solids holdup in the CFB regime*

The variation of the axial solids holdup distribution with primary liquid velocity at two different auxiliary liquid velocities is shown in Fig. 8a and b. It is evident from the figures that in the circulating fluidized bed regime, the solids holdup is uniformly distributed in the axial direction regardless of the primary and auxiliary liquid velocity. This observation is similar to that reported in literature [16,21].

The solids holdup decreases quickly with increasing primary liquid velocity up to 0.21 m/s and beyond that the change in solids holdup is very small, as evident from Fig. 8a. This is because, the distributor effect is small at low primary liquid velocity and hence the solid circulation rate is sensitive to primary liquid velocity.

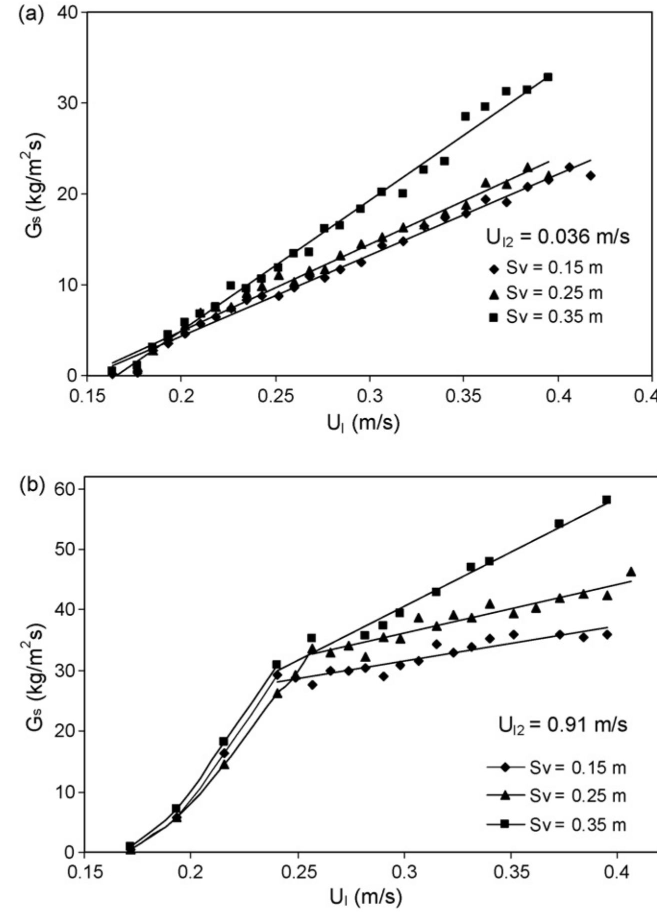

Fig. 7. (a) Effect of total solids inventory on particle circulation rate. (b) Effect of total solids inventory on particle circulation rate.

The axial distribution of solids holdup for different fixed total superficial liquid velocities and various combinations of auxiliary and primary liquid velocities is shown in Fig. 9a–d. For a fixed total superficial liquid velocity, axial distribution of solids holdup increases with increase in auxiliary liquid flow rate and at a fixed auxiliary liquid flow rate, the axial distribution of solids holdup decreases with increase in total superficial liquid velocity.

3.3. *Dynamic leak*

As mentioned earlier, the function of the auxiliary liquid is to mobilize the particles in the lift pot, push the solids to the tip of the tube and allow the particles into the riser from solids feeding pipe. The primary liquid acts as main fluidizing media for the solids pushed by the auxiliary liquid above the stainless steel tubes. When the column is operated with primary liquid alone (with no auxiliary liquid), no solids should enter the riser form the downcomer through the return leg and the solids circulation rate and solids holdup in the riser should be zero. During the initial experiments, the primary distributor was positioned in such a way that the upper tip of the stainless steel tubes were just 20 mm above the upper joint of riser and return leg (shown as position 1 in Fig. 4). When the primary liquid velocity is low (with no auxiliary liquid flow), the particles below the tubes are

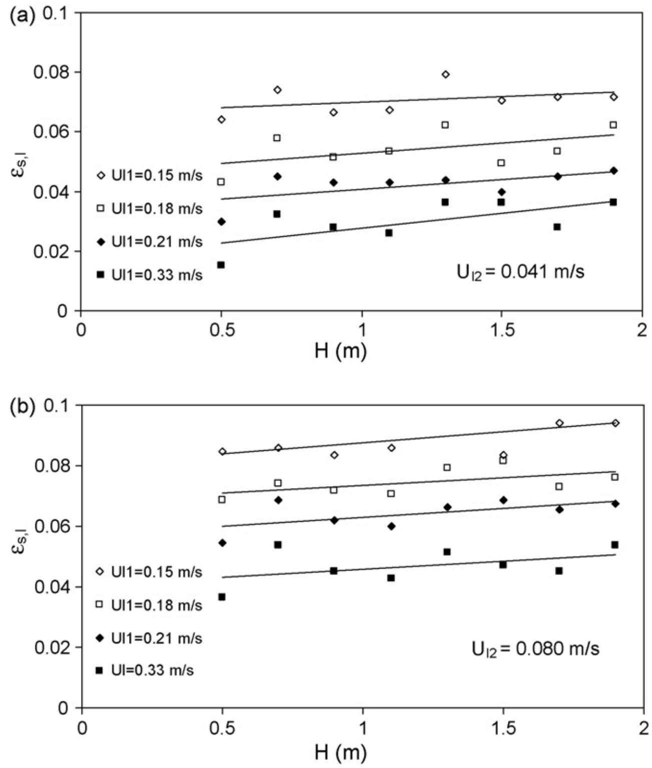

Fig. 8. (a) Variation of sectional solids holdup along the riser with axial position. (b) Variation of sectional solids holdup along the riser with axial position.

in packed bed and they cannot enter the riser. With increase in primary liquid velocity over a certain value (around 0.25 m/s), turbulence is created near the tip of the tubes. Liquid moves vigorously with wakes and pushes the solids that are adjacent to the tip of the tubes into the riser. Since the distance between the tip of the tubes and joint of the return leg and the riser is very less (20 mm) and because of turbulence, eddies are created near to the tip of the tubes. These eddies draw the solids from the upper part of return leg into the riser. Hence definite solids holdup and solids circulation rate are maintained in the riser. With further increase in primary liquid velocity, the distributor effect (that is turbulence action) will become more prominent. Additional solids are drawn from the return leg and solids circulation rate increases in the riser [26].

Hence, when primary liquid flow rate is above 0.25 m/s, solids flow from the solids feed pipe into the riser because of the position of the primary distributor and distributor effect. With further increase in the primary liquid velocity, more and more solids flow into the riser with the solids holdup increasing up to a certain liquid velocity and become constant beyond that. But the solids circulation rate increases continuously with main liquid velocity. This phenomenon is called dynamic leak. The maximum solids holdup (0.02) due to the dynamic leak at maximum main liquid velocity is less than that of transport bed regime [26].

The experimental procedure as described above was repeated for various solids inventories in the storage vessel by keeping the auxiliary liquid velocity to zero and varying the primary liquid velocity to a maximum. For every increment in primary liquid velocity, the solids holdup and solids circulation rate were noted down. For all the three solids inventories, the dynamic leak started around 0.25 m/s and the cross-sectional solids holdup and solids circulation rate are same at the same primary liquid velocity. From this it can be concluded that, with in the experimental range of solids inventory, the effect of solids inventory on the dynamic leak is negligible.

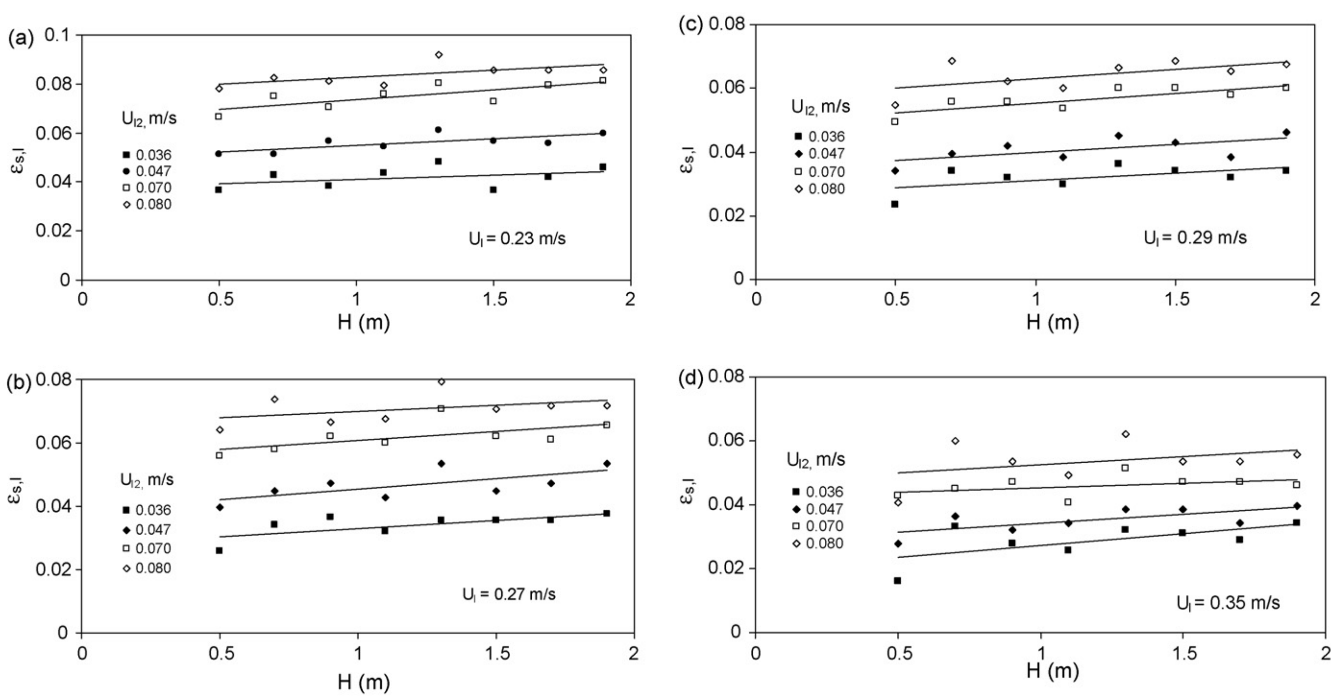

Fig. 9. (a) Variation of sectional solids holdup along the riser with axial position. (b) Variation of sectional solids holdup along the riser with axial position. (c) Variation of sectional solids holdup along the riser with axial position. (d) Variation of sectional solids holdup along the riser with axial position.

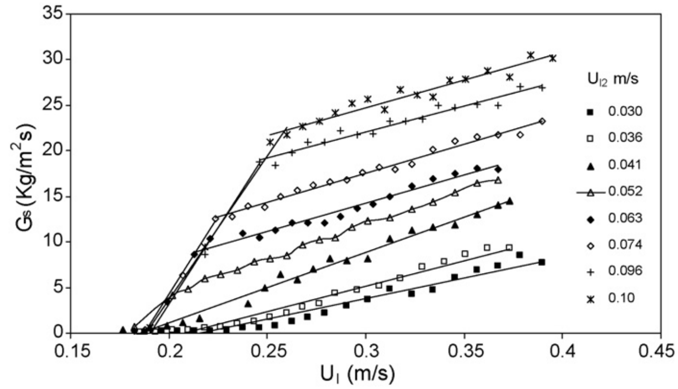

Fig. 10. Variation of solids circulation rate with liquid velocity without dynamic leak.

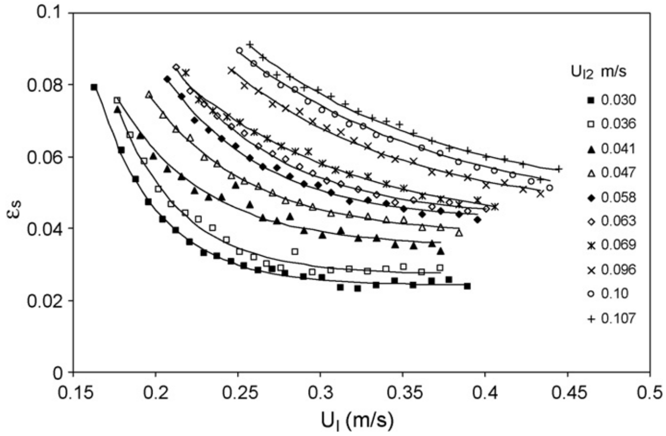

Fig. 11. Variation of solids circulation rate with liquid velocity without dynamic leak.

In normal operation of LSCFBs, both auxiliary and primary liquids are used. The liquid velocity just above the tubes is sum of the auxiliary and primary liquid velocities. At constant primary liquid velocity, the solids circulation rate and solids holdup contributed by auxiliary liquid velocity is different at different auxiliary liquid velocities (as shown in Figs. 3 and 5). In addition, the variation of average solids holdup and solids circulation rate with dynamic leak is not in linear with primary liquid velocity. Hence, it is difficult to quantify the contribution of leak by primary liquid velocity at various auxiliary liquid velocities. All the above results (shown in Figs. 2–9) are with dynamic leak, i.e. when the tip of the stainless steel tubes was at position 1 shown in Fig. 4.

In order to prevent this dynamic leak (otherwise the purpose of auxiliary distributor is not served), the height of the stainless steel tubes in the riser was increased. The increase in length of the tubes was based on the experiments conducted at maximum primary liquid velocity (decided the pump capacity) and noting down the height below the tip of the tubes that were affected due to turbulence created by the distributor. For the case without dynamic leak, the tube length in the riser is far away from the point of intersection of the riser and the return leg, shown as position 2 in the Fig. 4.

Experiments were repeated to identify the effect of dynamic leak on axial solids holdup distribution, average solids holdup and solids circulation rate for various constant auxiliary and primary liquid velocities and for different solid inventories.

Figs. 10 and 11, respectively, show the variation of solids circulation rate and average solids holdup with total superficial liquid velocity at various auxiliary liquid velocities. The increase in solids circulation rate is linear at low auxiliary liquid velocities and followed two zone phenomena at higher auxiliary liquid velocities. The trends are similar to Figs. 3 and 5. Similarly, Figs. 12 and 13, respectively, show the variation of solids holdup and solids circulation rate at two different auxiliary liquid velocities for different solids inventories. On comparison of Figs. 12 and 13 with Figs. 5 and 6, it can be concluded that the profiles are similar at both lower and higher auxiliary liquid velocities and the same phenomena hold with and without dynamic leak.

3.3.1. Comparison of flow behavior with and without dynamic leak

Fig. 14 compares the variation of the average solids holdup with and without dynamic leak at constant set of auxiliary liquid velocity and solid inventory. The solids holdup with dynamic leak is always higher than without due to the leak of solids form return leg into the riser at higher total liquid velocities. Fig. 15 shows the effect of dynamic leak on solids circulation rate. As before, a linear variation of solids circulation rate with superficial liquid velocity at lower U_{l2} and the two zone phenomena at higher auxiliary liquid velocities have been observed. The solids circulation rate is higher with dynamic leak than without. From Figs. 14 and 15, it can be concluded that the valve configuration is adding more restriction to solids to flow without dynamic leak than with dynamic leak and hence all the hydrodynamic variables in the case of without dynamic leak are lesser.

3.3.2. Variation of bed voidage with operating conditions

Fig. 16 shows the typical variation of bed voidage with solids circulation rate (expressed as superficial solids velocity) at various fixed superficial total liquid velocities. At a fixed U_l, the experimental voidage decreases with increasing solids circulation rate. The bed voidage, on the other hand, increases with increasing superficial liquid velocity at fixed superficial solids

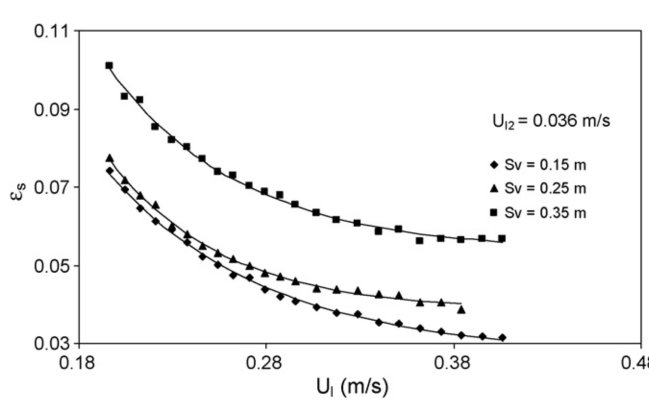

Fig. 12. Effect of total solids inventory on the solids holdup without dynamic leak.

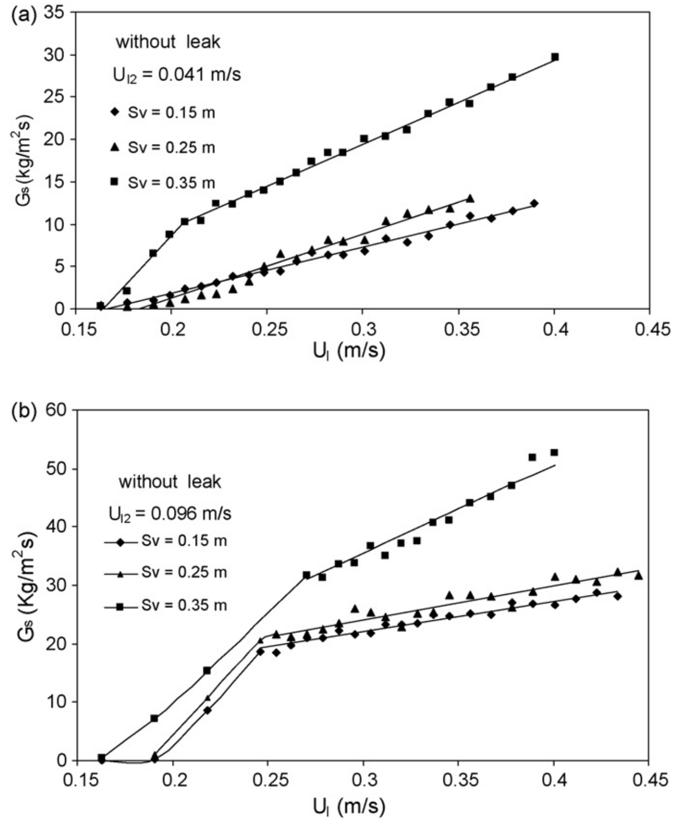

Fig. 13. (a) Effect of total solids inventory on the particle circulation rate. (b) Effect of total solids inventory on the particle circulation rate.

velocity. Hence the bed voidage can be determined by combining both solids circulation rate and superficial liquid velocity.

Assuming homogeneous fluidization in axial and radial directions, Kwauk [28] proposed the following relation between the voidage, superficial liquid velocity and superficial solids velocity by extending R-Z equation [27]:

$$\frac{U_l}{U_t} - \frac{U_s}{U_t}\frac{\bar{\varepsilon}}{1-\bar{\varepsilon}} = \bar{\varepsilon}^n \tag{1}$$

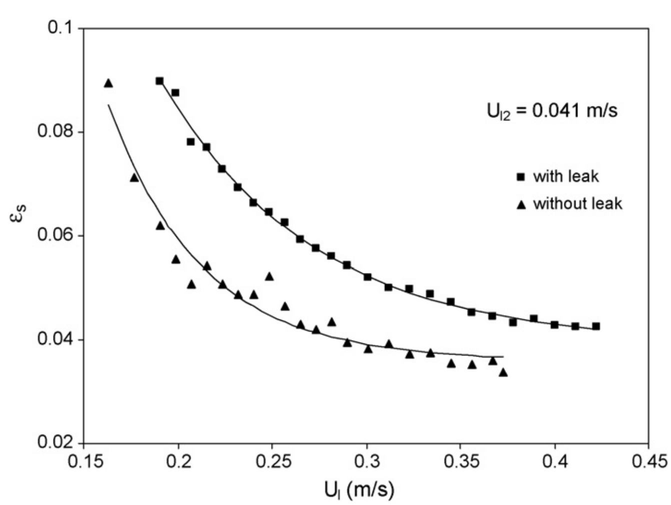

Fig. 14. Effect of dynamic leak on solids holdup.

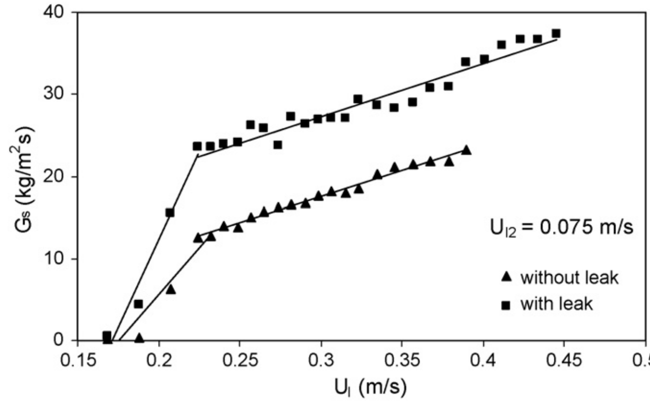

Fig. 15. Effect of dynamic leak on solid circulation.

The voidage predicted using the above equation is compared with experimental in Fig. 16. The predicted voidage is always higher than the experimental.

Similarly, it is observed that there is a significant difference in experimentally observed U_{slip}, C_{D} from that predicted by assuming homogenous fluidization. Hence correlations based on homogenous fluidization may not be readily applicable to the circulating fluidization regime because of difference in flow structure. These observations are similar to the reported literature [12,19].

3.4. Onset velocity experiments for regime transition identification

As the total superficial liquid velocity is varied, the bed in the riser will undergo different operating regimes. Since there is a significant difference in hydrodynamic behavior from one regime to other, it is of primary importance to know the critical liquid velocities which demarcates one regime from the other. There are three different methods to identify the critical transitional liquid velocity that demarcates the conventional and circulating fluidized bed regimes [15,17,29,30].

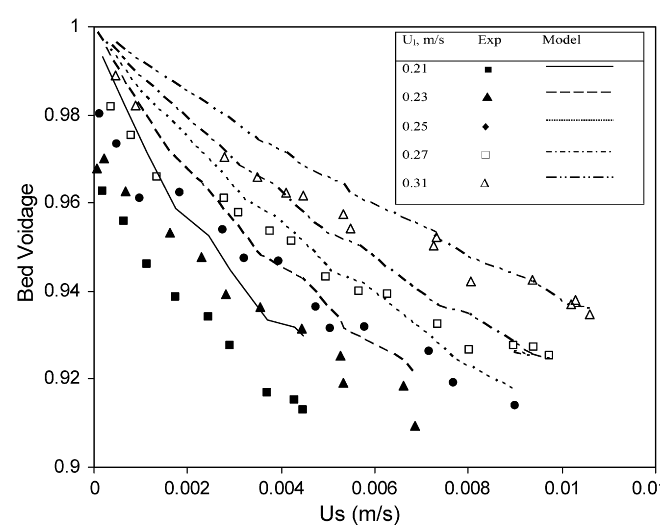

Fig. 16. variation of bed voidage with superficial particle velocity.

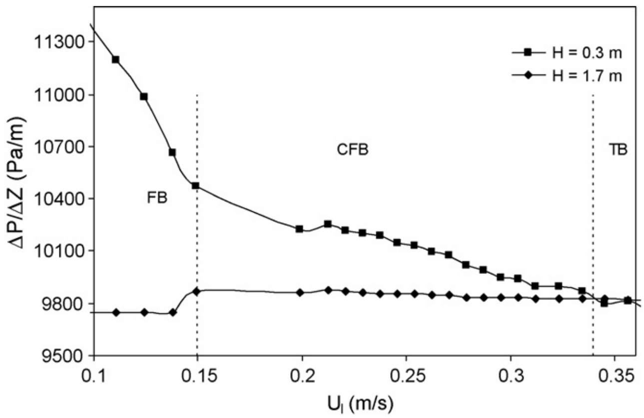

Fig. 17. Pressure drop as a function of superficial liquid velocity at two elevations.

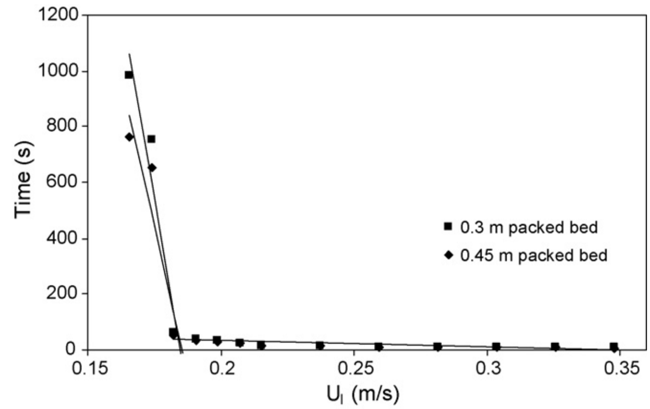

Fig. 18. Time taken to entrain solids in the riser as a function of liquid velocity.

3.4.1. Pressure gradient profile method

Fig. 17 shows the variation of pressure gradient plotted as a function of total superficial liquid velocity at two axial locations. The pressure gradient at lower section (at $H = 0.3$ m) decreases continuously with increasing liquid velocity due to dense phase expansion. On the other hand, at the upper section of the riser (at $H = 1.9$ m), the pressure gradient increases with increasing liquid velocity until a maximum is reached, i.e. up to $U_l = 0.15$ m/s. This means that the pressure gradient increases when the fluidizing solids enter that section; maximum pressure gradient is reached when entire uppermost section is occupied by the solids. With further increase in liquid velocity beyond 0.15 m/s, solids starts to entrain out from the section into the downcomer through liquid–solid separator and pressure gradient starts decreasing. So the peak in the pressure drop profile corresponds to a state of transition from conventional to CFB regime. Hence, the velocity at the peak of the pressure gradient line of top section is defined as the critical transitional velocity.

Vatanakul et al. [30] while studying on gas–liquid–solid system noted the range of critical transitional liquid velocity around 0.125–0.135 m/s which is less than that of the present study (0.15 m/s) even though the particle characteristics and geometry of riser of the present study ($d_p = 1.36$ mm, $\rho_s = 2468$ kg/m^3, $H = 2.2$ m, $D = 0.08$ m) are almost similar to them ($d_p = 1.3$ mm, $\rho_s = 2500$ kg/m^3, $H = 2.0$ m, $D = 0.076$ m). These authors have taken liquid velocity corresponds to maximum peak at elevation $H = 1.45$ m which really indicates the pressure gradient measured when the solids occupied up to 1.45 m from the bottom of the bed and rest of the section above the 1.45 m is free board region with no solids. So, the liquid velocity corresponds to maximum pressure gradient at the top most section very near to the exit of the riser must be considered as U_{lc}. Hence, U_{lc} obtained by them is less than that of the present study.

Similarly Zheng et al. [17] considered the liquid velocity corresponds to pressure peak at elevation of $H = 1.55$ m as U_{lc} (which means that when the solids are occupied up to height of 1.55 m solids are ready to entrain out of the riser) even though the height of the riser is 2.7 m.

3.4.2. Solids circulation method

The critical transitional velocity from conventional to circulating fluidized bed regime can be obtained from the plot of solids circulation rate as a function of superficial liquid velocity. As shown in Fig. 3, the velocity at which solids circulation rate changes form zero to non-zero is taken as the critical transitional liquid velocity.

3.4.3. Bed emptying method

As shown in Fig. 18, there exist two distinct lines with increasing superficial liquid velocity. At low total liquid velocity, the time taken for the particles to entrain is large as the interstitial liquid velocity (U_l/ε_l) is high and the particles entrain quickly with continuous decrease in solids holdup in the riser. As the time progresses, the interstitial liquid velocity decreases continuously and hence longer lengths time are needed to empty the particles. On the other hand, at higher total liquid velocities, interstitial liquid velocity is higher than the terminal velocity of a particle and hence it takes short time to entrain the particles with almost no particles in the riser. The onset velocity can be located at the point of intersection of the two lines.

Since the onset velocity is determined without solids storage vessel and solid feeding structure, it is independent of total solids inventory or structure of the feeding system. In addition, the onset velocity obtained by two initial static beds (0.3 and 0.45 m) is same; it is also independent of initial volume of the particles in the riser. Of all the methods, the determination of onset velocity by regime transition method is preferred because of simplicity and ease of the experiment.

The critical transitional and onset velocities obtained by the above methods are shown in the Table 2. The transitional velocity obtained by the pressure drop profile is lesser since the liq-

Table 2
The onset and critical transitional velocities obtained in the present study

Critical transitional velocity (m/s)		Onset velocity (m/s)
By pressure gradient profile method	By solids circulation rate method	By bed emptying method
0.15	0.163	0.182

uid velocity is not noted when the solids occupy the topmost measuring section.

4. Conclusions

In addition to operating conditions, such as primary and auxiliary liquid velocity, the non-mechanical valve configuration (i.e. angle made by the solids return pipe with the riser and the distance between the auxiliary distributor and the joint of solids return pipe with the riser), location of the primary liquid distributor and solids inventory in the storage vessel play an important role on the macroscopic properties of LSCFB. Solids circulation rate and solids holdup were found to increase with increase in auxiliary liquid velocity. Under constant set of primary and auxiliary liquid velocity, the solids circulation rate and solids holdup increase with increase in solid inventory in the downcomer. The solids circulation rate, the average solids holdup and the axial solids holdup distribution is always higher with dynamic leak than without dynamic leak. The experimental correlations developed based on the homogenous fluidization in expanded regime are found to be inapplicable to the circulating fluidized bed regime. Hence a new strategy is needed to model the flow characteristics in circulating fluidized bed regime.

Acknowledgement

The authors gratefully acknowledge Prof. J.-X. Zhu, Department of Chemical Engineering, University of Western Ontario, Canada for his valuable discussion and suggestions on dynamic leak during his visit to India.

References

[1] J.-X. (Jesse) Zhu, Y. Zheng, D.G. Karamanev, A.S. Bassi, (Gas)–liquid–solid circulating fluidized beds and their potential applications to bioreactor engineering, Can. J. Chem. Eng. 78 (2000) 82–94.
[2] W. Liang, Z. Yu, Y. Jin, Z. Wang, Y. Wang, Synthesis of linear alky benzenes in a liquid–solid circulating fluidized bed reactor, J. Chem. Technol. Biotechnol. 62 (1995) 98–102.
[3] W.G. Liang, J.-X. Zhu, Radial flow non-uniformity on the alkylation reaction in a liquid–solid circulating fluidized bed (LSCFB) reactor, Ind. Eng. Chem. Res. 36 (1997) 4651–4658.
[4] C. Xu, M. Han, S. Chen, J. Wang, Y. Jin, Reactor modeling of innovative liquid–solid circulating moving bed for the synthesis of linear alkyl benzenes, Chem. Eng. Commun. 191 (2004) 796–812.
[5] S. Chen, M. Han, C. Xu, D. Wang, Y. Jin, Structure optimization of a circulating moving bed reactor, Chem. Eng. Commun. 192 (2005) 1598–1620.
[6] S. Roy, A. Kemoun, M.H. Al-Dahhan, M.P. Dudukovic, Experimental investigation of hydrodynamics in a liquid–solid riser, AIChEJ 51 (2005) 802–835.
[7] Q. Lan, J.-X. (Jesse) Zhu, A.S. Bassi, A. Margaritis, Y. Zheng, G.E. Rowe, Continuous protein recovery using a liquid–solid circulating fluidized bed ion exchange system: modelling and experimental studies, Can. J. Chem. Eng. 78 (2000) 858–866.
[8] Q. Lan, A.S. Bassi, J.-X. (Jesse) Zhu, A. Margaritis, Continuous protein recovery with a liquid–solid circulating fluidized-bed ion exchanger, AIChEJ 48 (2002) 252–261.
[9] Q. Lan, A.S. Bassi, J.-X. (Jesse) Zhu, A. Margaritis, Continuous protein recovery from whey using liquid–solid circulating fluidized bed ion-exchange extraction, Biotechnol. Bioeng. 78 (2002) 157–163.
[10] Y. Cui, G. Nakhla, J. Zhu, A. Patel, Simultaneous carbon and nitrogen removal in anoxic-aerobic circulating fluidized bed biological reactor (CFBBR), Environ. Technol. 25 (2005) 699–712.
[11] L.-S. Fan, Gas–Liquid–Solid Fluidization Engineering, Butterworth Publishers, MA, 1989.
[12] W. Liang, S. Zheng, J.-X. Zhu, Y. Jin, Z. Yu, Z. Wang, Flow characteristics of the liquid–solid circulating fluidized bed, Powder Technol. 90 (1997) 95–102.
[13] Y. Zheng, J.-X. (Jesse) Zhu, Z. Wen, S.A. Marting, A.S. Bassi, A. Margaritis, The axial hydrodynamic behavior in a liquid–solid circulating fluidized bed, Can. J. Chem. Eng. 77 (1999) 284–290.
[14] Y. Zheng, J.-X. (Jesse) Zhu, Overall pressure balance and system stability in a liquid–solid circulating fluidized bed, Chem. Eng. J. 79 (2000) 145–153.
[15] Y. Zheng, J.-X. (Jesse) Zhu, The onset velocity of a liquid–solid circulating fluidized bed, Powder Technol. 114 (2001) 244–251.
[16] Y. Zheng, J.-X. Zhu, N.S. Marwaha, A.S. Bassi, Radial solids flow structure in a liquid–solid circulating fluidized bed, Chem. Eng. J. 88 (2002) 141–150.
[17] Y. Zheng, J. Zhu, A. Wushouer, Transition from low velocity to high velocity in a three phase fluidized bed, Chem. Eng. Technol. 28 (2005) 1010–1015.
[18] X. Feng, S. Jing, Q. Wu, J. Chen, C. Song, The hydrodynamic behavior of the liquid–solid circulating fluidized bed ion exchange for cesium removal, Powder Technol. 134 (2003) 235–242.
[19] K. Kuramoto, K. Tanaka, A. Tsutsumi, K. Yoshidha, T. Chiba, Macroscopic flow structure of solid particles in circulating liquid–solid fluidized bed riser, J. Chem. Eng. Jpn. 31 (1998) 258–265.
[20] S. Roy, A. Kemoun, M. Al-Dahhan, M.P.D. Dudukovic, A method for estimating the solids circulation rate in a closed-loop circulating fluidized bed, Powder Technol. 121 (2001) 213–222.
[21] S. Roy, M.P. Dudukovic, Flow mapping and modeling of liquid–solid risers, Ind. Eng. Chem. Res. 40 (2001) 5440–5454.
[22] Y. Zheng, Radial particle profiles in a liquid–solid CFB with varying viscosity, Chem. Eng. Technol. 27 (2004) 769–776.
[23] W.G. Liang, Q. Wu, Z. Yu, Y. Jin, Z. Wang, Hydrodynamics of a gas–liquid–solid three phase circulating fluidized bed, Can. J. Chem. Eng. 73 (1995) 656–661.
[24] W.G. Liang, Q.W. Wu, Z.Q. Yu, Y. Jin, H.T. Bi, Flow regimes of the three-phase circulating fluidized bed, AIChEJ 41 (1995) 267–271.
[25] Y.J. Cho, P.S. Song, S.H. Kim, Stochastic analysis of gas–liquid–solid flow in three-phase circulating fluidized beds, J. Chem. Eng. Jpn. 34 (2001) 254–261.
[26] J.-X. (Jesse) Zhu, Personal communication, 2006.
[27] J.F. Richardson, W.N. Zaki, Trans. Inst. Chem. Eng. 32 (1954) 35.
[28] M. Kwauk, in: J. Wei (Ed.), Advances in Chemical Engineering, vol. 17, Academic Press, Sandiego, 1991, p. 207.
[29] J. Adanez, L.F. de Diego, P. Gayan, Transport velocities of coal and sand particles, Powder Technol. 77 (1993) 61–68.
[30] M. Vatanakul, Y. Zheng, L. Jia, K. Zhang, Regime transition in a gas–liquid–solid fluidized bed, Chem. Eng. J. 108 (2005) 35–45.